Evaluation of an Al-Zn-Mg-Li Alloy/Potential Candidate as Al-Sacrificial Anode

S. Valdez, J. Genesca, B. Mena, and J.A. Juarez-Islas

(Submitted 22 March 2000; in revised form 5 June 2000)

This paper forms part of an overall effort to develop Al-sacrificial In/Hg free anodes; our research has been directed toward developing Al alloys appropriate for cathodic protection. The Al-Zn-Mg system has been particularly selected due to the presence of precipitates in the α-Al matrix, which are capable of breaking down passive films while presenting good electrochemical efficiencies. At the same time, the effect of Li additions on superficial activation of the anode by means of precipitation of AlLi-type compounds was examined. The microstructure was characterized in the as-cast and as-aged ingots, showing the presence of α-Al dendrites as well as eutectic of $Al_2Mg_3Zn_3$ and precipitates of Mg_7Zn_3 in interdendritic regions. Electron microscopic observations performed on specimens with and without heat treatments showed in the α-Al matrix the presence of a uniform distribution of precipitates of (τ-$Al_2Zn_3Mg_3$, Mg_7Zn_3, and δ-AlLi type. The electrochemical behavior of the alloy was investigated in a 3% NaCl solution simulating seawater at room temperature. After evaluation of the electrochemical efficiency, values up to 67% were obtained. The relationship between microstructure and electrochemical efficiency is discussed in this work and suggestions of future research are given in order to improve the electrochemical behavior of Al anodes in the field.

Keywords Al-sacrificial anodes, electrochemical efficiency, microstructure, precipitates

1. Introduction

Presently, the most commonly used sacrificial metals for cathodic protection systems are alloys of Mg, Zn, and Al. The Al anodes are keenly related to alloy chemistry and to environmental application. Aluminum has attained considerable merit as the basis for a galvanic anode mainly due to its low density, large electrochemical equivalent, availability, and reasonable cost. The low electrode potentials of Al anodes are readily adaptable to a variety of saline environments such as seawater, marine muds, and brackish waters. Unalloyed Al adopts a relatively noble solution potential in saline media as a result of its protective oxide film. The oxide is the cause of rapid polarization when aluminum is placed under a corrosion load in a cathodic protection circuit. Nevertheless, the success of the Al anode depends upon the alloying of certain metals whose surface role is to ultimately prevent the formation of a continuous, adherent, and protective oxide film on the alloy, thus permitting continuous galvanic activity of the aluminum. Research carried out toward the development of Al alloys appropriate for cathodic protection has considered the influence of alloying elements such as Zn, Ti, Hg, and In.[1,2] The use of each of those elements has shown an improvement of Al activation in neutral chloride media. However, the seemingly good results obtained in this field are in contrast with the increased sensitivity to environmental protection. Particularly, the use of In alone or coupled with Hg in Al alloys during dissolution results in sea life pollution and gives rise to great environmental issues. In order to avoid sea life pollution due to elements such as Hg and In, and at the same time provide an Al alloy adequate for cathodic protection application, the Al-Zn-Mg system has been investigated in terms of distribution of intermetallics in the α-Al matrix capable of breaking down passive films as well as presenting good electrochemical efficiencies.[3] Regarding electrochemical efficiency or anode current capacity, this should be expressed in A-h/kg (where A-h is ampere-hour) and represents a figure of the effectiveness of the anode alloy. The electrochemical capacity is often expressed as percent of efficiency.

For instance, it has been reported,[4] in the as-cast condition, the existence of a microstructure consisting of α-Al solid solution with precipitation of the τ phase and a eutectic consisting of a fine dispersion of the $\alpha + \tau$ segregated at grain boundaries. Further dispersion of the τ phase in the matrix has been increased by means of thermal treatments applied to as-cast ingots, by taking advantage of the fast kinetic reactions taking place in solid state at 400 °C, giving as a result Al anodes with electrochemical efficiencies up to 78%.[5]

This research has as its main scope to identify the possibility of the substitution of Al-Zn-In and Al-Zn-In-Hg sacrificial anodes, by alloys of the Al-Zn-Mg type, in order to avoid sea life pollution without decreasing the current efficiency of the resulting anodes. The first part of this research was focused on the identification and distribution of precipitates in the Al alloy, in order to achieve two targets: the first one is to obtain a good surface activation of the anode and the second to yield corrosion products similar to those found in seawater in order to avoid pollution of sea life. As a first step, reference was made of the work of Barbucci[5] producing Al-Zn-Mg alloys but with

S. Valdez, B. Mena, and **J.A. Juarez-Islas,** Instituto de Investigaciones en Materiales-UNAM, Circuito Escolar S/N, Cd. Universitaria, 04510, Mexico, D.F. Mexico; and **J. Genesca,** Fac. de Quimica, Depto de Metalurgia-UNAM, Circuito Escolar S/N, Cd. Universitaria. Contact e-mail: julioalb@servidor.unam.mx.

additions of Li. The resulting microstructure was then characterized, with particular attention paid to identification of precipitates in the α-Al matrix and eutectics in interdendritic regions, in both as-cast ingot and aged samples. The research was also directed toward the effect of Li additions on superficial activation of the anode by means of precipitation of the δ-AlLi intermetallic at grain boundaries and/or matrix, and by taking advantage of the fact that the Zn decreases the solid solubility of Li in the α-Al phase.[6]

2. Experimental Procedure

An Al-5 at.% Zn-5 at.% Mg-0.1 at.% Li alloy was prepared with commercially available Al, Zn, and Mg with purities of 99.98%. The Li was used as a wire of 3.2 mm in diameter and 99.9% of purity with 4.5 mg/cm of Na. Due to previous experiences during melting of these kinds of alloys and in order to avoid losses of Mg, Zn, and Li, these elements were placed in Al capsules. Initially, the Al was placed in an alumina/graphite coated crucible and melted in a resistance furnace under an argon atmosphere. Once the Al was melted, the liquid bath was overheated 150 °C and the Al capsules containing Zn and Mg were added. The bath was stirred with argon for 10 min in order to have uniform distribution of Zn and Mg. Immediately after this operation, the Al capsule containing Li was added to the liquid bath, which was stirred with a flux of argon for another 5 min after which the liquid alloy was poured into a copper mold of dimensions $8 \times 8 \times 50$ cm. The top and bottom of the ingot were cut off for chemical analysis, giving a nominal composition of Al-4.8 at.% Zn-5.1 at.% Mg and 0.09 at.% Li.

In order to perform the characterization of the resulting microstructure, the ingots were sectioned transversally to the heat flow, ground, polished, and etched in Keller's reagent to reveal the different phases, precipitates, and/or intermetallic compounds present in the ingot. Aged treatments were performed in the as-cast ingot in order to enhance precipitation, following the aging steps (1) aging at 400 °C for 5 h and (2) aging at 400 °C for 5 h with an additional heating of 160 °C for 2 h. The resulting microstructure was characterized using a Stereoscan 440 scanning electron microscope (SEM, Leica Electron Optics, England) and a 2100 Jeol scanning transmission electron microscope (STEM, Japan Electron Optics, Tokyo). Both electron microscopes were equipped with wavelength dispersive x-ray (WDX) microanalyses facilities. X-ray diffractometry on aluminum samples in all conditions was performed using a Siemens 5000 x-ray diffractometer with Cu K_α radiation, a Ni filter, and a scan velocity of 2°/min.

A laboratory procedure was carried out for determining the current capacity characteristics of the new aluminum alloy. A sample of dimensions $1 \times 1 \times 0.2$ cm of the Al alloy was electrically connected to a steel screen cathode forming a galvanic pair with a cathode/anode area ratio of 50:1 and immersed in a 3% NaCl solution at ambient temperature for 45 days. A 500 cm^3 plastic container was filled with the NaCl solution and used as the anode test cell. Anode current capacity was determined by weight loss. The total current that passed through the system was measured by a coulometer. Anode weight loss was determined at the end of the 45 day test when the samples were removed, cleaned, and weighed. Weight loss current capacities are thus determined from knowledge of the total charge passed through the system and the weight loss of the anode sample.

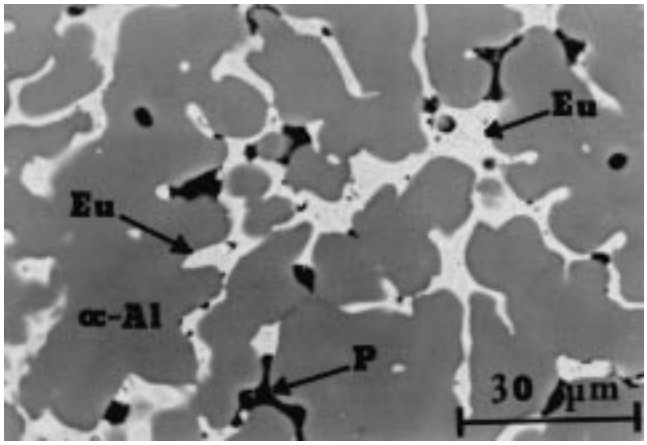

Fig. 1 As-cast microstructure of the Al-Zn-Mg ingot

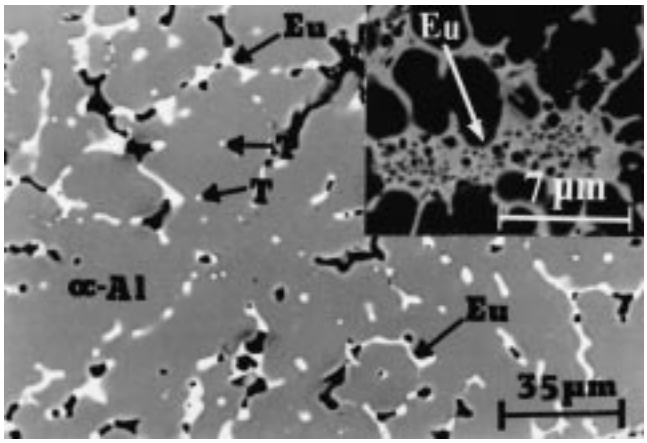

Fig. 2 Microstructure observed in samples aged at 400 °C (5 h). Inset shows the coarsening and growth of the spherical particles aligned as rows in the eutectic

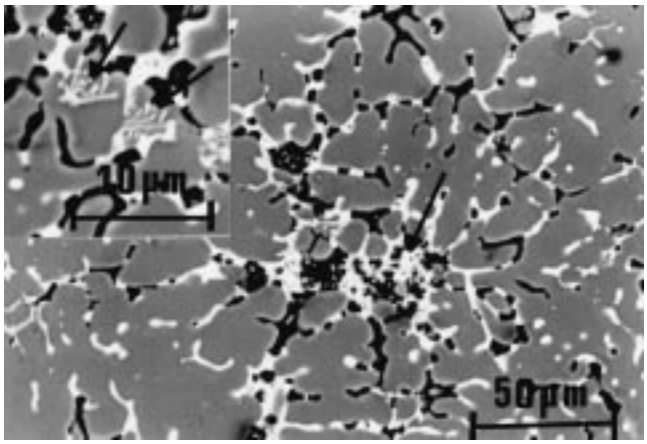

Fig. 3 Microstructure observed in samples aged at 400 °C (5 h) with an additional heating of 160 °C (2 h). Inset shows the development of a dendrite-like morphology in the eutectic

3. Results and Discussion

A representative microstructure observed in the as-cast ingot, as shown in Fig. 1, consisted of α-Al dendrites with sizes between 130 to 150 μm. In the interdendritic regions, the presence of eutectic and black spherical particles was observed. The eutectic showed a white color with a maximum width of 10 μm, always following the contour of the dendritic arms. This eutectic, instead of presenting a platelet morphology as that reported in Ref 5, showed the presence of rows formed by gray spherical particles.

Figure 2 shows the microstructure observed in samples aged at 400 °C (5 h). The dendritic structure was modified, giving place to the coarsening of primary and secondary arms. The white eutectic (with a maximum width of 7 μm) started to migrate toward future grain boundaries, leaving traces of the interdendritic species in the α-Al matrix, which takes the morphology of spherical particles. Also, it was observed that the spherical particles present as rows inside the white eutectic started to growth (inset in Fig. 2). The black spherical particles located at a secondary, dendritic arm spacing did not show any change at this stage.

In order to evaluate the effect of a secondary aging treatment, the samples aged at 400 °C for 5 h received an additional aging treatment a 160 °C for 2 h more. The observed microstructure under this aging condition is shown in Fig. 3, where there appears to be an increase in the amount of black spherical particles following the contours of the secondary dendritic arms. The width of the space occupied by the black spherical particles increased from 2 μm (in the as-cast ingot) to ~6 μm (in this aging stage). Also, an additional feature was observed in regions of the eutectic that correspond to the development of a dendrite-like pattern (inset in Fig. 3).

In order to qualitatively identify the species present in the as-cast ingot and in the aged specimens, x-ray diffractometry was applied; and, from the collected data, seven peaks were detected in each condition. As expected, the main peaks corresponded to the α-Al phase. Also, the presence of binary precipitates of MgZn, Mg_4Zn_7, Mg_7Zn_3, $MgZn_2$, AlMg, Al_3Mg_2, $Mg_{17}Al_{12}$, Al_4Li_9, LiZn, and AlLi were detected; ternary precipitates of $AlMg_4Zn_{11}$, Al_2MgLi, LiMgZn, and $Al_2Mg_3Zn_3$ and quaternary precipitates of $Al_{0.9}Li_{34.3}Mg_{64.5}Zn$ and $Al_{0.9}Li_{34.3}Mg_{64.5}Zn$ also appeared. The kind of precipitates and their respective *d*-spacings are shown in Table 1. An interesting feature of these x-ray diffractograms was an increase in the relative intensity (I/I_o) of peaks II, III, and VII for both aged conditions, indicating, from a qualitative point of view, the precipitation of particles containing Li.

In addition, WDX microanalyses were carried out in specimens in both as-cast and as-aged conditions (Table 2). For example, in the as-cast specimens, it was possible to retain 4.7 at.% Zn and 4.2 at.% Mg in α-Al solid solution. The Li was not detected due to the characteristics of the detector.

In the first as-aged condition (400 °C, 5 h), the amount of

Table 1 Phases and compounds identified by x-ray diffraction

	As cast		Aged(a)		Aged(b)		
Peak	***d* (Å)**	***I*/*I*$_o$**	***D* (Å)**	***I*/*I*$_o$**	***d* (Å)**	***I*/*I*$_o$**	**Phases**
I	2.340	100	2.334	100	2.344	100	α-Al, MgZn, Mg_4Zn_7, Mg_7Zn_3, AlMg, Al_3Mg_2, Al_4Li_9, $AlMg_4Zn_{11}$
II	2.028	19	2.023	53	2.028	35	α-Al, $AlMg_4Zn_{11}$, Al_2MgLi
III	1.434	44	1.432	49	1.435	54	α-Al, MgZn, $MgZn_2$, $Mg_{17}Al_{12}$, LiZn, LiMgZn, Al_3Mg_2
IV	1.224	38	1.223	38	1.224	14	α-Al, AlMg, AlLi
V	1.172	5	1.171	4	1.172	4	$Al_{0.9}Li_{34.3}Mg_{64.5}Zn$
VI	0.932	6	0.932	12	0.932	5	α-Al, $Al_{0.7}Zn_{0.3}$, $Al_2Mg_3Zn_3$
VII	0.908	4	0.906	19	0.906	12	AlLi, $Al_{0.7}Zn_{0.3}$, $Al_{0.9}Li_{34}Mg_{64}Zn$, $Al_2Mg_3Zn_3$

(a) Aged at 400 °C, 5 h
(b) Aged at 400 °C with an additional heating of 160 °C for 2 h

Table 2 WDX microanalyses results of as-cast and aged specimens (in at.%)

Condition (→) **Microstructure (↓)**		**As cast (at.%)**	**Aged(a) (at.%)**	**Aged(b) (at.%)**
α-Al dendrites	Al	91.00 ± 2.0	…	…
	Mg	4.20 ± 0.50	3.50 ± 0.50	3.50 ± 0.10
	Zn	4.70 ± 0.20	3.22 ± 0.65	4.00 ± 0.15
White eutectic	Al	41.00 ± 3.0	39.00 ± 4.0	41.00 ± 3.0
	Mg	32.00 ± 1.0	33.00 ± 2.0	32.00 ± 2.5
	Zn	27.00 ± 3.0	28.00 ± 1.5	27.00 ± 3.6
Black particles	Al	…	…	…
	Mg	71.00 ± 2.0	72.00 ± 2.50	70.00 ± 4.00
	Zn	29.00 ± 6.0	28.00 ± 4.0	29.00 ± 2.00

(a) Aged at 400 °C, 5 h
(b) Aged at 400 °C with an additional heating of 160 °C for 2 h

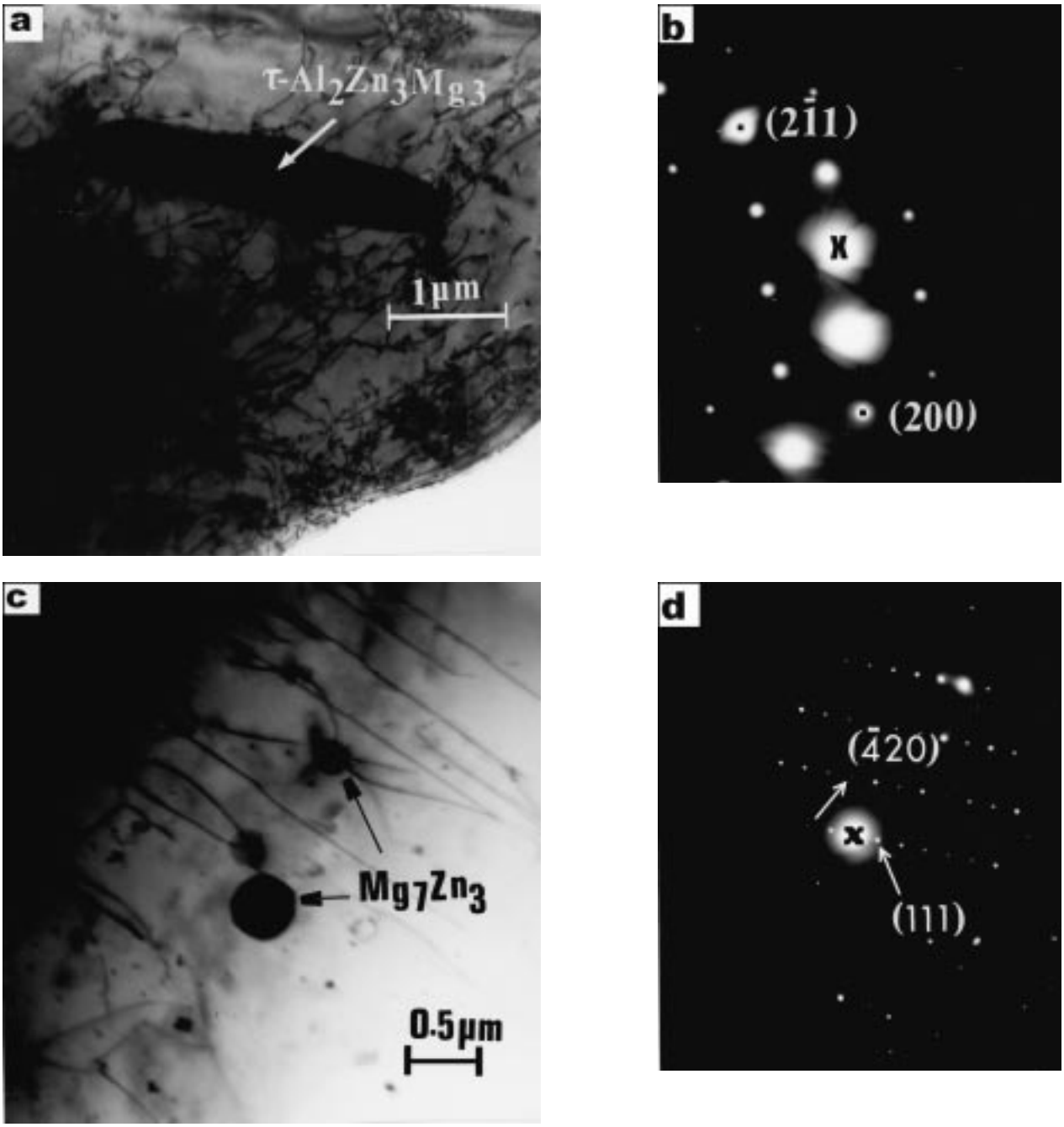

Fig. 4 (**a**) A photomicrograph of the specimen in the as-cast condition where the presence of a platelet-like precipitate is observed. (**b**) Selected area diffraction pattern of τ-$Al_2Zn_3Mg_3$ phase. (**c**) Spherical precipitates of Mg_7Zn_3. (**d**) Selected area diffraction pattern of the Mg_7Zn_3 phase

Zn and Mg present in the α-Al solid solution decreased. This decay in both elements was attributed to the coarsening of the eutectic located in interdendritic regions. Regarding composition of this eutectic, the amount of Mg detected was in the range of 32 to 33 at.% and the amount of Zn was in the range of 27 to 28 at.%, the remaining being Al. As mentioned before, the black spherical particles observed in the interdendritic regions did not present any change, and their composition was almost constant, corresponding to precipitates of Mg_7Zn_3. In the second aging stage, an increase in the amount of black particles in the interdendritic region was observed, with an almost constant composition. The only detected change in composition corresponded to the transition of the eutectic to a dendritelike precipitate, whose composition corresponded to Al-16.6 at.% Zn-13.25 at.% Mg with a contamination of 3.3 at.% Fe.

The TEM observations were performed in the specimens with and without heat treatment in order to identify the main species present in the α-Al matrix. Figure 4(a) shows a photomicrograph of the specimen in the as-cast condition, where the

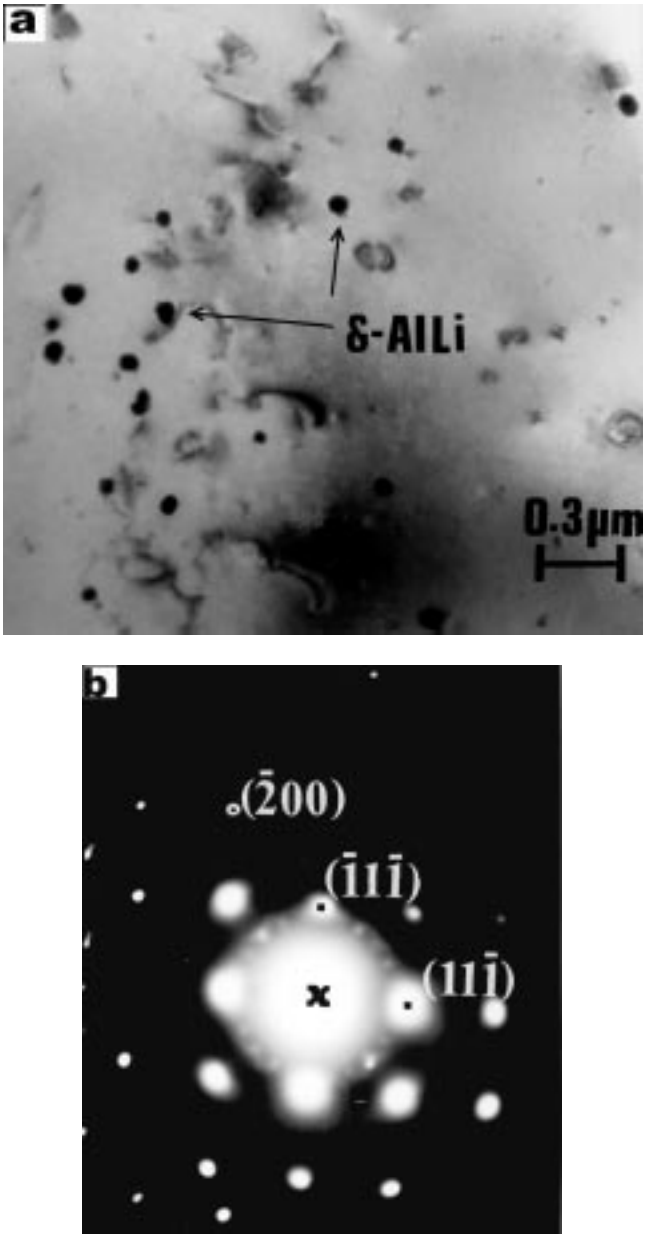

Fig. 5 (**a**) Morphology of precipitates rich in lithium. (**b**) Selected area diffraction pattern of the δ-AlLi precipitates

presence of a platelet-like precipitate of about 1800 nm in length may be observed. Spherical precipitates (40 to 200 nm), linked by dislocations, are shown in Fig. 4(c). Selected area diffraction patterns taken in those precipitates identified them as the intermetallic τ-$Al_2Zn_3Mg_3$ (Fig. 4b) and Mg_7Zn_3 (Fig. 4d). In both aged conditions, besides detecting the presence of precipitates of the τ-$Al_2Zn_3Mg_3$ and the Mg_7Zn_3 type, the presence of a precipitate rich in lithium was also detected, as shown in Fig. 5(a). This was identified by its selected area diffraction pattern as δ-AlLi (Fig. 5b), with an average size of 80 nm.

Regarding the electrochemical behavior in terms of efficiency of the as-cast ingot and aged samples, it can be said that the efficiency of the as-cast ingot showed an average value of 62%, while the efficiency of aged samples at 400 °C (5 h) showed an average value of 67%, and the aged sample at 400 °C for 5 h with an additional heating of 160 °C for 2 h showed an average value of 65%.

It should be mentioned that recent research directed toward the development of aluminum sacrificial anodes of the Al-Mg-Zn type reported[5] values of electrochemical efficiency between 63 and 78% (−1082 mV; SCE). These results were attributed to a good dispersion of the τ phase[7] in the α-Al matrix, which was reached by a long-term aging treatment (400 °C, 24 h), being the intermetallic compound responsible for the breakdown of the passive film and at the same time leading to a quite generalized dissolution. When additions of In, Ga, and Ca were made to the Al-Mg-Zn alloy,[8] and the resulting alloy was thermally treated at 500 °C (4 h), the Al anodes reached efficiencies up to 95.6% (−1090 mV; SCE). This excellent value of efficiency was attributed to a homogeneous distribution of Ga and a precipitation of In and Ca. Therefore, the research has shifted to the production of Al alloys, which can show high electrochemical efficiencies. To reach that goal, during the present research, the as-cast microstructure must be improved in order to increase the electrochemical efficiency of Al anodes by means of decreasing or eliminating the presence of Mg_7Zn_3 precipitates in interdendritic regions. The reason for moving to this direction is that, during dissolution of the Al anode, the Mg_7Zn_3 particles did not dissolve. This provokes the isolation of some α-Al dendrites, giving place to a localized pitting corrosion mechanism and at the same time decreasing the electrochemical efficiency of the Al anode. On the other hand, it was detected that precipitates of the τ-$Al_2Zn_3Mg_3$ and δ-AlLi type played an important role in terms of breaking down the aluminum oxide passive film, permitting at the same time a continued galvanic activity and an increase of the electrochemical efficiency of the Al anode.

4. Conclusions

- The resulting Al-Zn-Mg-Li alloy showed two kinds of species in the interdendritic spacing, which corresponded to a eutectic of $Al_2Zn_3Mg_3$ and precipitates of Mg_7Zn_3.
- By means of TEM observations, the presence of the τ-$Al_2Mg_3Zn_3$ intermetallic compound, precipitates of Mg_7Zn_3, and δ-AlLi precipitation in the α-Al matrix were identified, the presence of those species for the activation of the aluminum electrode being relevant by means of passive film breakdown, which can lead to a quite generalized dissolution of the Al anode.
- In order to improve the electrochemical efficiency of the Al anode, it was apparent that research must be focused toward the role played by the τ-$Al_2Zn_3Mg_3$, Mg_7Zn_3, and δ-AlLi compounds in the α-Al matrix, and toward the effect of the decay of the eutectic and particles in interdendritic regions. This will result in the prevention of the formation of a continuous, adherent, and protective oxide film by particle precipitation, leading to a uniform dissolution of the Al anode.

Acknowledgments

The authors are grateful for the financial support by DGAPA, Grant No. IN109398. The participation of Mr. E. Caballero and Eng. L. Baños is also gratefully acknowledged.

References

1. A.R. Despic: *J. Appl. Electrochem.*, 1976, vol. 6, p. 499.
2. M. Salleh: Ph.D. Thesis, UMIST, Manchester, United Kingdom, 1978.
3. J.B. Clark: *Trans. Am. Soc. Met.*, 1961, vol. 53, p. 295.
4. G.M. Kuznetsov and A.D. Barsukov: *Izv. Akad. Nauk, SSSR Met.*, 1986, vol. 4, p. 198.
5. A. Barbucci, G. Cerisola, G. Bruzzone, and A. Saccone: *Electrochem. Acta*, 1997, vol. 42, p. 2369.
6. R.J. Kilmer and G.E. Stonere: *Light Weight Alloys for Aerospace Applications II*, TMS, Warrendale, PA, 1991, p. 3.
7. D.A. Petrov: in *Ternary Alloys*, G. Petzow and G.E. Effemberg, eds., 1993, vol. 7, p. 57.
8. X. Zhand and Y. Wang: *Corr. Sci. Protection*, 1995, vol. 7 (1), p. 53.